Supplementary Information for

Interfacial water shuffling the intermediates of hydrogen oxidation and evolution reactions in aqueous media

Ershuai Liu[1], Li Jiao[2], Jingkun Li[1,3], Thomas Stracensky[1], Qiang Sun[1], Sanjeev Mukerjee[1], and Qingying Jia*[,1]

[1]Department of Chemistry and Chemical Biology, Northeastern University, Boston, Massachusetts, 02115, United States

[2]Department of Chemical Engineering, Northeastern University, Boston, Massachusetts, 02115, United States

[3]Institut Charles Gerhardt Montpellier, UMR 5253, CNRS, Université Montpellier, ENSCM, Place Eugène Bataillon, 34095 Montpellier cedex 5, France

[1] is the previous address of J.L.; [3] is the present address.
*Correspondence authors. q.jia@northeastern.edu (Q. J.)

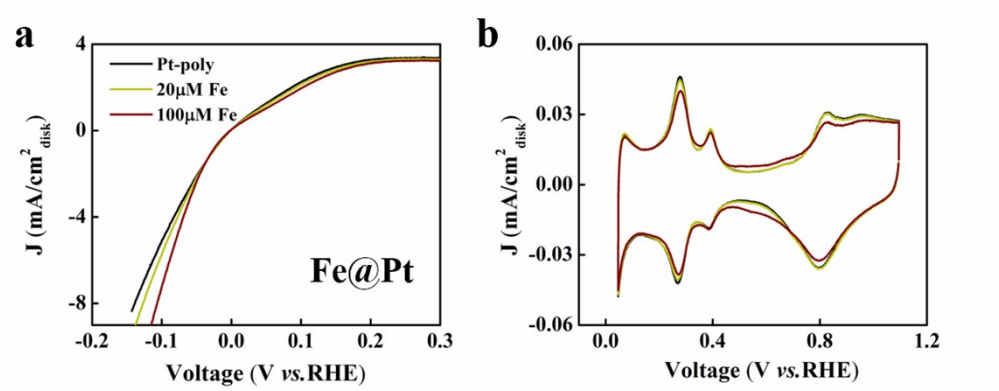

Figure S1. (a) *IR*-corrected HOR/HER polarization curves collected at room temperature in an H_2-saturated 0.1 M KOH electrolyte on the Pt polycrystalline electrode with Fe^{3+}. Scan rate: 10 $mV \cdot s^{-1}$. Rotation rate: 2,500 rpm. **(b)** The *CV* collected at room temperature in an Ar-saturated 0.1 M KOH electrolyte on the Pt polycrystalline electrode with varied concentrations of Fe^{3+}. Scan rate: 20 $mV \cdot s^{-1}$.

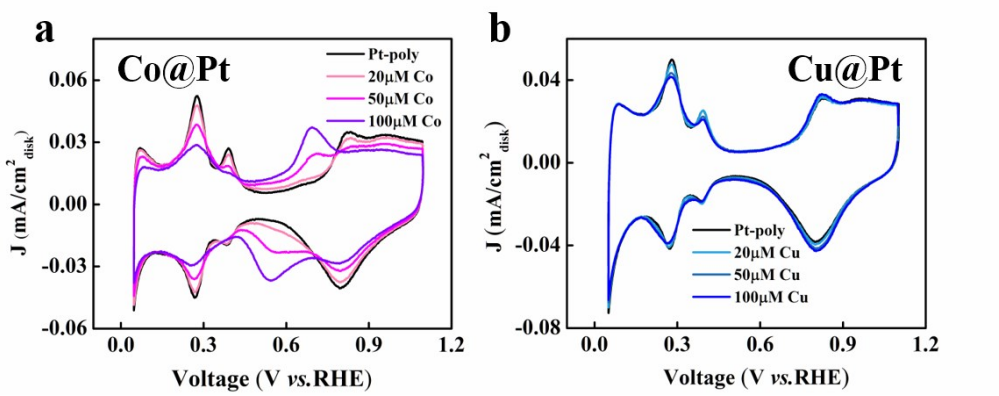

Figure S2. The CV collected at room temperature in an Ar-saturated 0.1 M KOH electrolyte on the Pt polycrystalline electrode with varied concentrations of Co^{2+} (**a**) and Cu^{2+} (**b**). Scan rate: 20 $mV \cdot s^{-1}$.

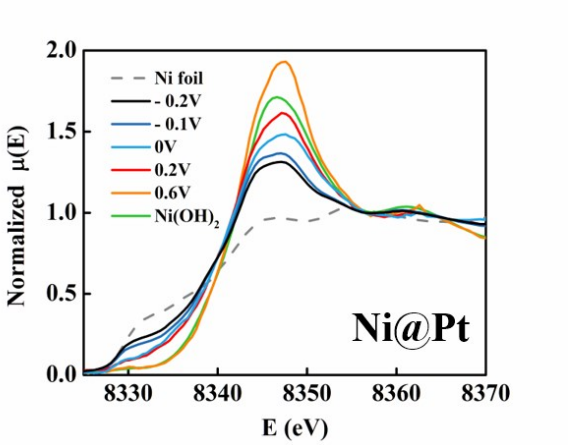

Figure S3. The K-edge XANES spectra of the Ni@Pt as a function of applied potentials collected in an H_2-purged 0.1 M KOH electrolyte. Some of the data were obtained from our previous work (Ref 15).

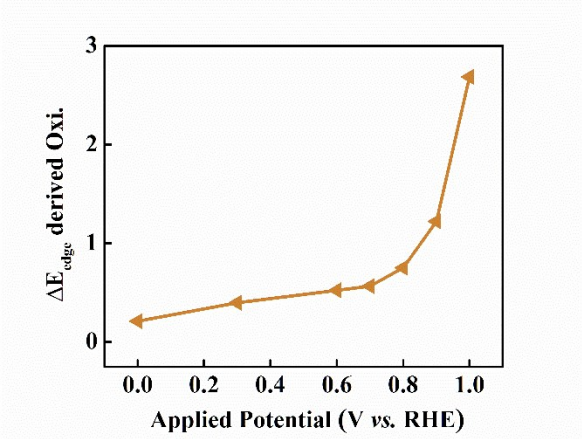

Figure S4. The oxidation states of Ru/C derived from the E_{edge} of the XANES spectra (**Figure 2e**) as a function of applied potentials.

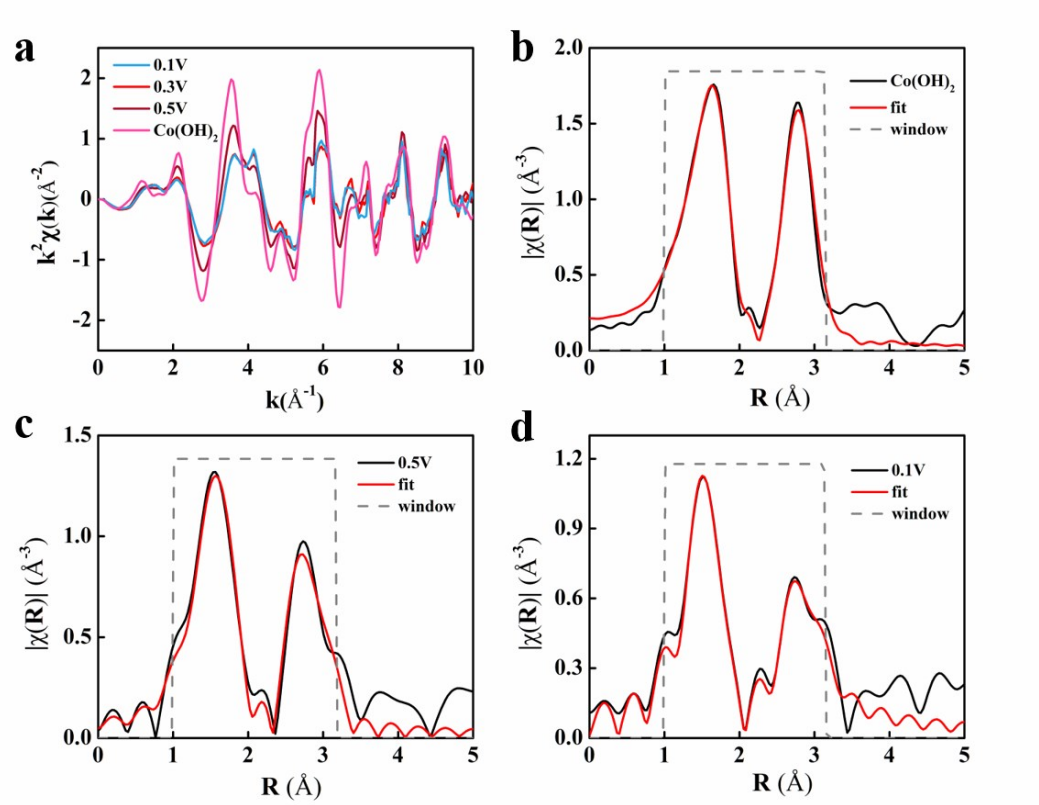

Figure S5. The *in situ* EXAFS spectra at the Co K-edge of Co@Pt and $Co(OH)_2$ at both the k **(a)** and R **(b-d)** spaces, together with the corresponding EXAFS fitting.

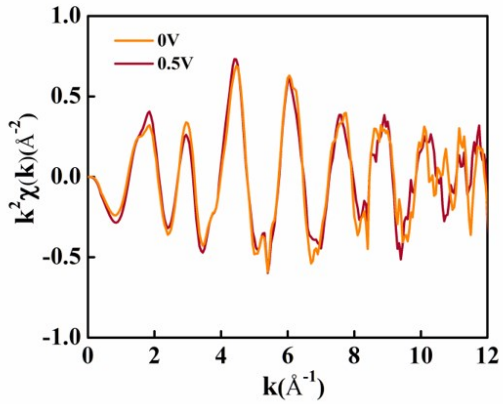

Figure S6. The *in situ* FT-EXAFS spectra at the Cu K-edge of Cu@Pt at the k space.

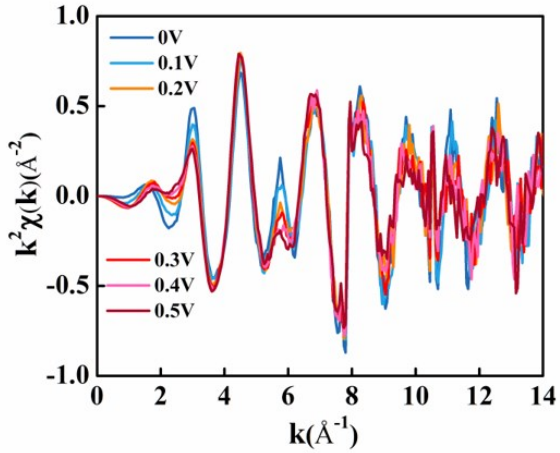

Figure S7. The *in situ* FT-EXAFS spectra at the Ru K-edge of Ru@Pt at the k space.

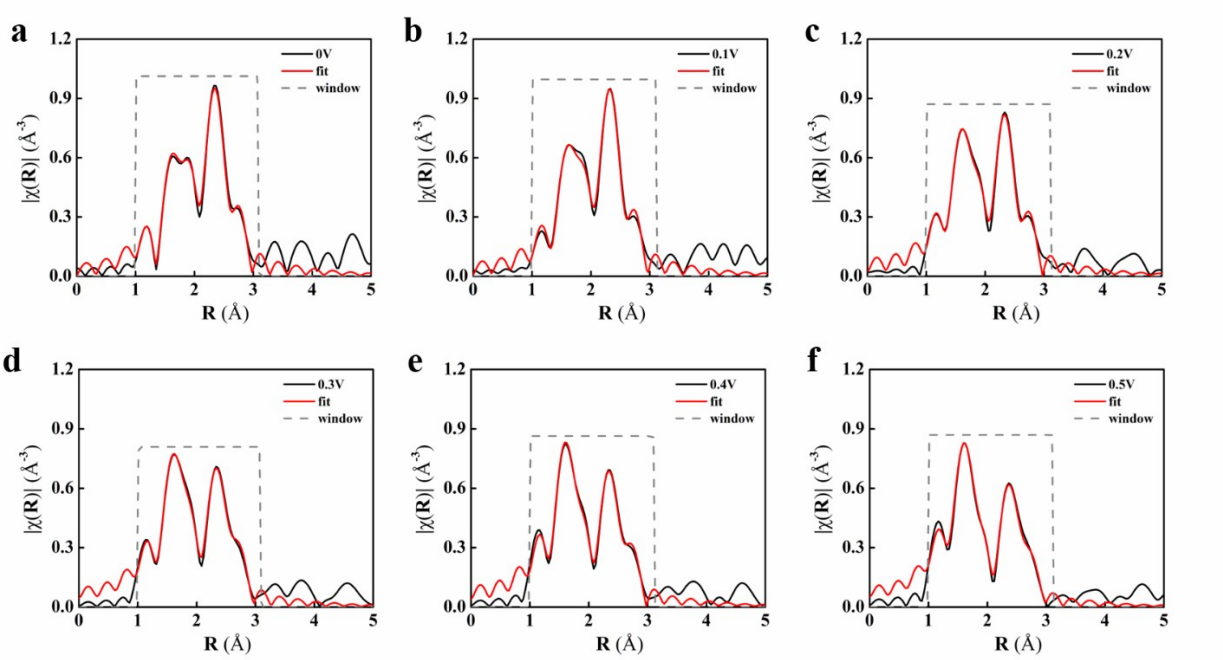

Figure S8. The *in situ* FT-EXAFS spectra at the Ru K-edge of Ru@Pt within 0 – 0.5 V, together with the corresponding EXAFS fittings.

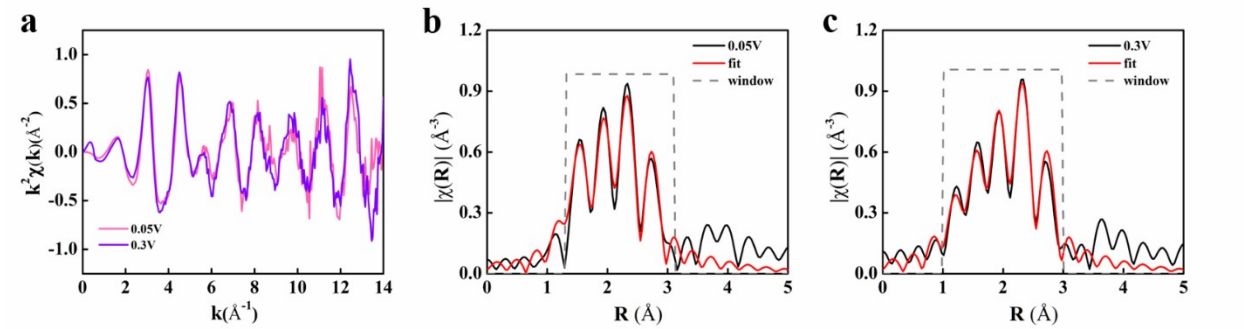

Figure S9. The *in situ* FT-EXAFS spectra at the Ru K-edge of the Pt_1Ru_1/C at both the k **(a)** and R **(b-c)** spaces, together with the corresponding EXAFS fitting.

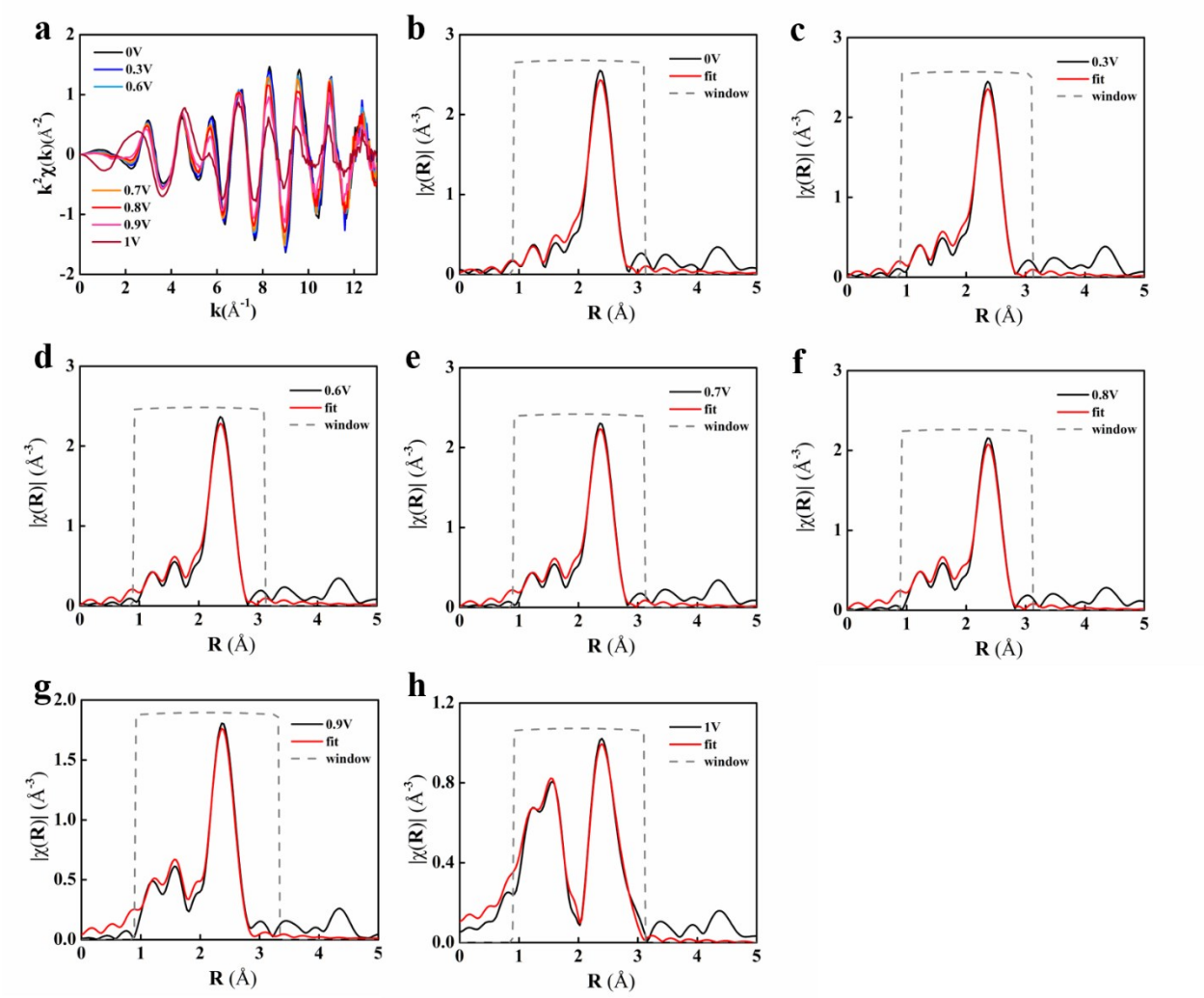

Figure S10. The *in situ* FT-EXAFS spectra at the Ru K-edge of Ru/C at both the k **(a)** and R **(b-c)** spaces, together with the corresponding EXAFS fitting (**d-h**).

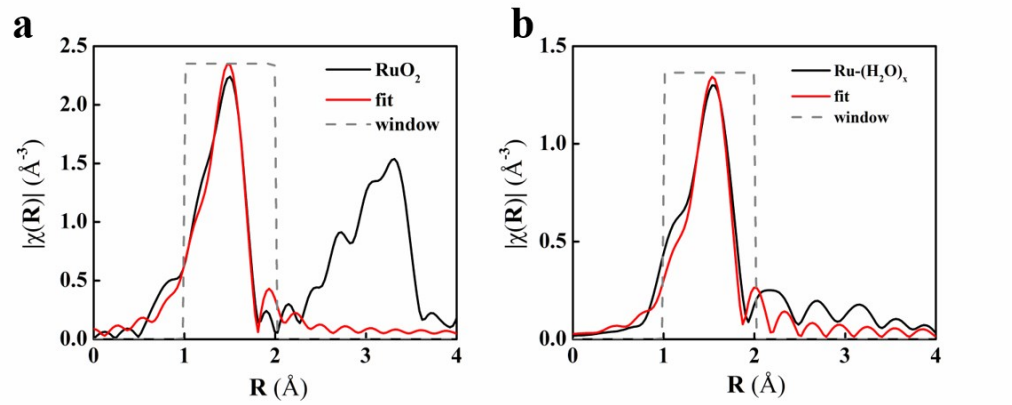

Figure S11. The *ex situ* FT-EXAFS spectra at the Ru K-edge of RuO_2 **(a)** and $RuCl_3$ **(b)** solution (denoted as Ru-$(H_2O)_x$) at the R space, together with the corresponding EXAFS fitting.

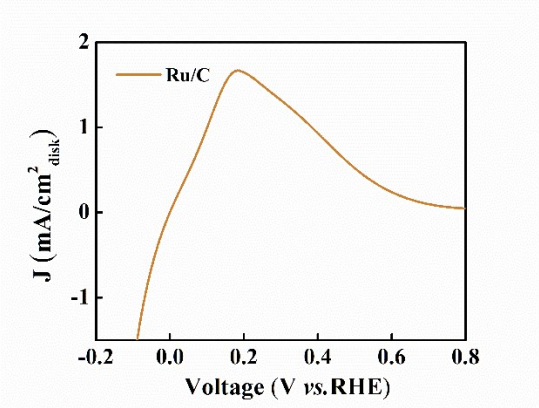

Figure S12. The *iR*-corrected HOR/HER polarization curves collected at room temperature in an H_2-saturated 0.1 M KOH electrolyte of Ru/C. Scan rate: 10 mV·s^{-1}. Rotation rate: 2,500 rpm.

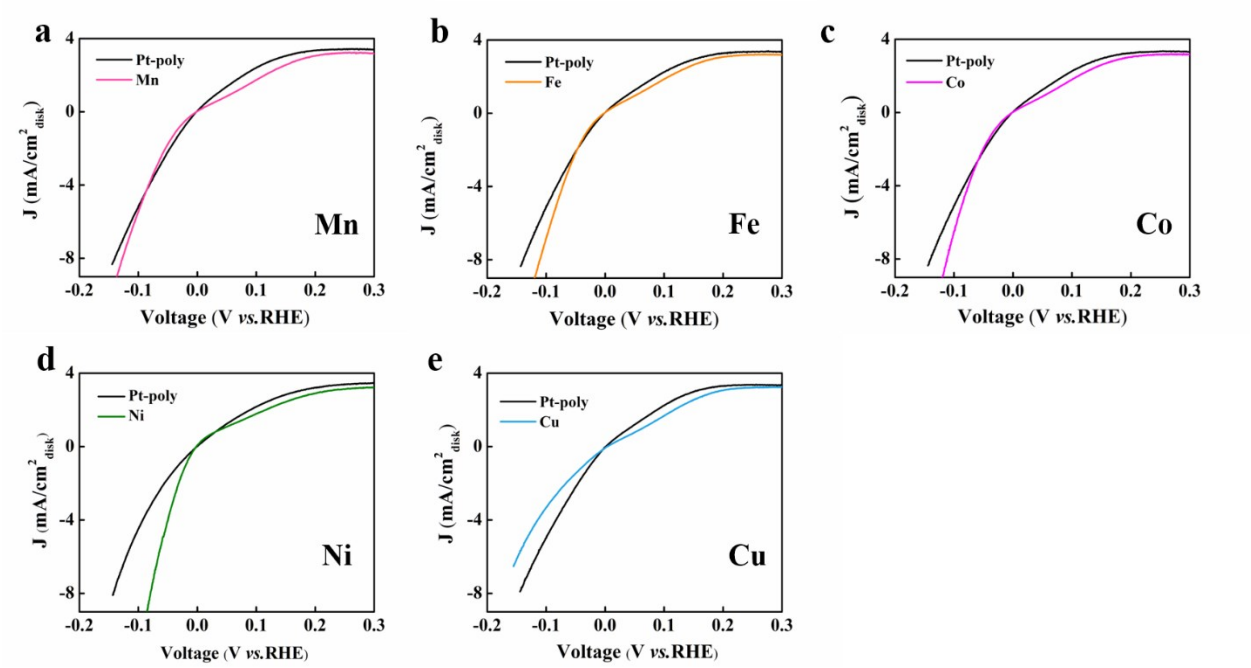

Figure S13. The iR-corrected HOR/HER polarization curves collected at room temperature in an H_2 -saturated 0.1 M KOH electrolyte on the Pt polycrystalline electrode with Mn^{2+} **(a)**, Fe^{3+} **(b)**, Co^{2+} **(c)**, Ni^{2+} **(d)** and Cu^{2+} **(e)**. TM coverage is 30% ~ 40%. Scan rate: 10 mV·s $^{-1}$. Rotation rate: 2,500 rpm.

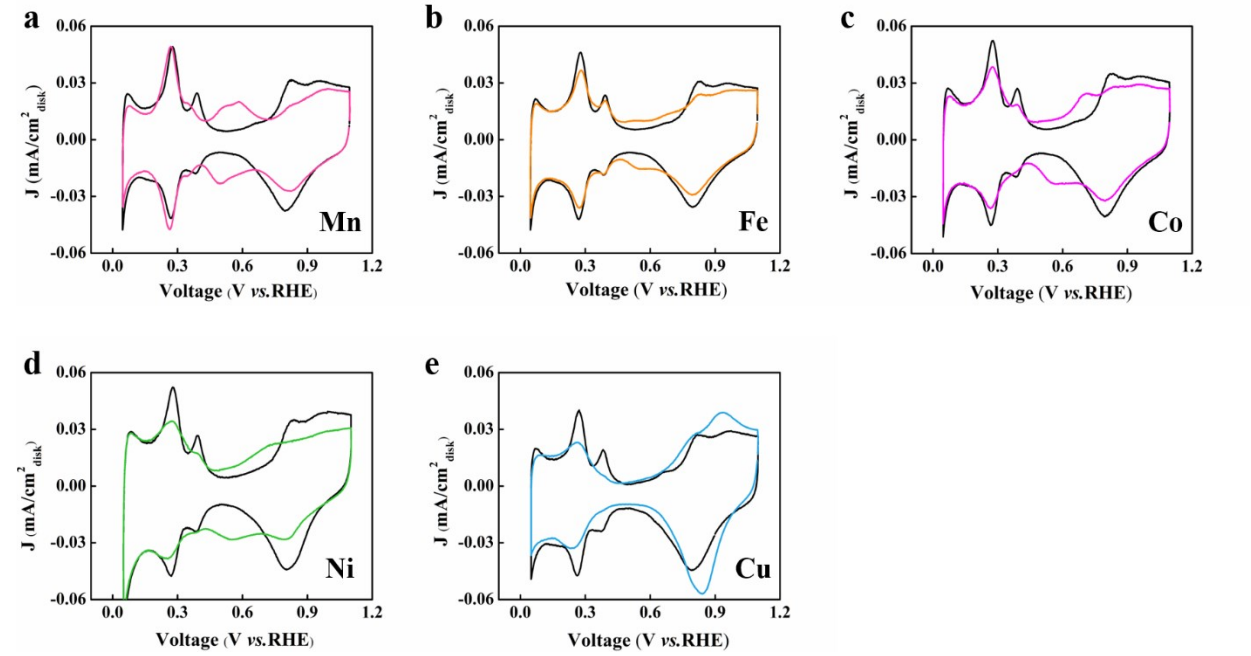

Figure S14. The *CV*s collected at room temperature in an Ar-saturated 0.1 M KOH electrolyte on the Pt polycrystalline electrode with Mn^{2+} (**a**), Fe^{3+} (**b**), Co^{2+} (**c**), Ni^{2+} (**d**) and Cu^{2+} (**e**). TM coverage is 30% ~ 40%. Scan rate: 20 mV·s^{-1}.

Table S1. Summary of the fitting results of the FT-EXAFS spectra collected at the Co K-edge of the Co@Pt in a H_2-saturated 0.1 M KOH electrolyte, together with that of the $Co(OH)_2$ std.

Paths	Co-O			Co-Co			
	R (Å)	N	$\sigma^2 \times 10^{-3}$ (Å^2)	R (Å)	N	$\sigma^2 \times 10^{-3}$ (Å^2)	E_0 (eV)
0.1 V	2.05(3)	3(1)	3(2)	3.19(1)	2(1)	3(3)	-1(1)
0.5 V	2.07(2)	3.9(7)	6(3)	3.18(1)	3(1)	4(3)	0.3(9)
$Co(OH)_2$	2.10(1)	6.2(4)	7(1)	3.18(1)	7(1)	7(2)	1.0(6)

*Fits were done at the Co K-edge in *R*-space, $k^{1,2,3}$ weighting. $1.0 < R < 3.16$ Å and $\Delta k = 2.63 – 12.86$ Å^{-1} for $Co(OH)_2$ and $\Delta k = 2.63 – 9.95$ Å^{-1} for Co@Pt owing to the noisy spectra at the high k region were used for fitting. S_0^2 was fixed at 0.95 obtained by fitting the reference Co foil. The number given in the parentheses represents the uncertainty of the last digit of the fitting result.

Table S2. Summary of the fitting results of the FT-EXAFS spectra collected at the K-edge of the Ru@Pt in a H_2-saturated 0.1 M KOH electrolyte*

Path	Ru-O_s			Ru-O_l			Ru-Ru			Ru-Pt		
	R (Å)	N	$\sigma^2 \times 10^{-3}$ (Å^2)	R (Å)	N	$\sigma^2 \times 10^{-3}$ (Å^2)	R (Å)	N	$\sigma^2 \times 10^{-3}$ (Å^2)	R (Å)	N	$\sigma^2 \times 10^{-3}$ (Å^2)
0 V	1.79(3)	0.6(6)	3(3)	2.03(2)	1.9(9)	3(3)	2.65(1)	4.2(7)	5(1)	2.67(2)	2.7(7)	5(1)
0.1 V	1.80(3)	0.6(3)	2(2)	2.02(1)	1.9(4)	2(2)	2.63(1)	4.2(6)	5(1)	2.67(2)	2.7(6)	5(1)
0.2 V	1.81(4)	0.7(3)	1(3)	2.02(1)	2.1(8)	1(3)	2.64(1)	3.7(3)	5	2.67(1)	2.7(5)	5
0.3 V	1.80(2)	0.9(3)	3(2)	2.02(1)	2.8(7)	3(2)	2.64(1)	3.4(3)	5	2.66(1)	3.0(5)	5
0.4 V	1.80(3)	0.9(2)	2(2)	2.02(1)	2.7(5)	2(2)	2.65(1)	3.3(3)	5	2.67(1)	2.9(4)	5
0.5 V	1.80(2)	1.1(2)	2(1)	2.01(1)	2.9(3)	2(1)	2.65(1)	2.9(3)	5	2.67(1)	2.8(5)	5

*Fits were done at the Ru K-edge in *R*-space, $k^{1,2,3}$ weighting. $1.0 < R < 3.1$ Å and $\Delta k = 2.63 – 12.86$ Å^{-1} were used for fitting. S_0^2 was fixed at 0.80 obtained by fitting the reference Ru foil. The number given in the parentheses represents the uncertainty of the last digit of the fitting result. The fitting results of the E_0 are: -3±1 eV (0 V), -4±1 eV (0.1 V), -4±1 eV (0.2 V), -4±1 eV (0.3 V) -4±1 eV (0.3 V), -4±1 eV (0.4 V), -4±1 eV (0.5 V).

Table S3. Summary of the fitting results of the FT-EXAFS spectra collected at the K-edge of the Ru in the Pt_1Ru_1/C in a H_2-saturated 0.1 M KOH electrolyte.*

Path	Ru-O_s			Ru-O_l			Ru-Ru			Ru-Pt		
	R (Å)	N	$\sigma^2 \times 10^{-3}$ (Å^2)	R (Å)	N	$\sigma^2 \times 10^{-3}$ (Å^2)	R (Å)	N	$\sigma^2 \times 10^{-3}$ (Å^2)	R (Å)	N	$\sigma^2 \times 10^{-3}$ (Å^2)
0.05 V	-	-	-	2.00(2)	1.2(4)	3	2.66(1)	3.6(7)	4(1)	2.70(1)	3.9(9)	4(1)
0.3 V	1.82(4)	0.7(4)	3	2.01(3)	1.3(6)	3	2.66(1)	3.8(4)	4	2.70(1)	4.0(7)	4

*Fits were done at the Ru K-edge in *R*-space, $k^{1,2,3}$ weighting. $1.0 < R < 3.1$ Å and $\Delta k = 2.63 – 12.86$ Å^{-1} were used for fitting. S_0^2 was fixed at 0.80 obtained by fitting the reference foil. The number given in the parentheses represents the uncertainty of the last digit of the fitting result. The fitting results of the E_0 are: -3±1 eV (0 V), -5±1 eV (0.3 V).

Table S4. Summary of the fitting results of the FT-EXAFS spectra collected at the Ru K-edge of the Ru/C in a H_2-saturated 0.1 M KOH electrolyte*

Path	Ru-O_s			Ru-O_l			Ru-Ru^0			Ru-Ru^{3+}		
	R (Å)	N	$\sigma^2 \times 10^{-3}$ (Å^2)	R (Å)	N	$\sigma^2 \times 10^{-3}$ (Å^2)	R (Å)	N	$\sigma^2 \times 10^{-3}$ (Å^2)	R (Å)	N	$\sigma^2 \times 10^{-3}$ (Å^2)
0 V	1.81(4)	0.7(7)	3	2.03(4)	0.9(8)	3	2.65(1)	6(1)	4(1)	3.01(3)	1.4(6)	4(1)
0.3 V	1.80(4)	0.8(6)	3	2.01(4)	1.2(7)	3	2.65(1)	6(1)	4(1)	3.02(2)	1.4(6)	4(1)
0.6 V	1.81(4)	0.8(5)	3	2.00(3)	1.3(7)	3	2.66(1)	6(1)	4(1)	3.02(2)	1.7(5)	4(1)
0.7 V	1.80(3)	0.8(5)	3	2.00(2)	1.3(6)	3	2.66(1)	6(1)	4(1)	3.02(2)	1.8(5)	4(1)
0.8 V	1.81(3)	1.0(6)	3	2.01(3)	1.7(7)	3	2.67(1)	6(1)	5(1)	3.03(3)	1.6(6)	5(1)
0.9 V	1.81(3)	1.0(5)	3	1.99(2)	1.7(5)	3	2.66(1)	5(1)	5(1)	3.03(2)	1.7(5)	5(1)
1.0 V	1.81(2)	1.6(5)	3	1.98(1)	3.0(5)	3	2.66(1)	3(1)	5	3.03(2)	2.6(5)	5

*Fits were done at the Ru K-edge in *R*-space, $k^{1,2,3}$ weighting. $1.0 < R < 3.0$ Å and $\Delta k = 2.63 – 12.86$ Å^{-1} were used for fitting. S_0^2 was fixed at 0.84 obtained by fitting the reference foil. The number given in the parentheses represents the uncertainty of the last digit of the fitting result. The fitting results of the E_0 are: -4±1 eV (0 V), -4±1 eV (0.3 V), -4±1 eV (0.6 V), -5±1 eV (0.7 V) -4±2 eV (0.8 V), -5±2 eV (0.9 V), -5±2 eV (1.0 V). Ru-Ru^0 and Ru-Ru^{3+} represents the Ru-Ru bonds in the metallic Ru and $Ru(OH)_3$ phases, respectively.

Table S5. Summary of the fitting results of the FT-EXAFS spectra collected at the K-edge of the Ru in the RuO_2 standard and the $RuCl_3$ solution (0.1 M)*

	Ru-O			
	R (Å)	N	$\sigma^2 \times 10^{-3}$ (Å^2)	E_0 (eV)
RuO_2	1.97(1)	6(1)	2(1)	1(1)
$RuCl_3$ solution	2.04(1)	5(1)	1(2)	-1(1)

*Fits were done at the Ru K-edge in *R*-space, $k^{1,2,3}$ weighting. $1.0 < R < 2.0$ Å and $\Delta k = 2.63 – 12.86$ Å^{-1} (RuO_2) and $\Delta k = 2.63 – 11.75$ Å^{-1} ($RuCl_3$ solution) were used for fitting. S_0^2 was fixed at 0.80 obtained by fitting the reference foil. The number given in the parentheses represents the uncertainty of the last digit of the fitting result.

Table S6. Summary of the three categories of Pt-based catalysts and the corresponding reaction mechanisms.

	Representative catalysts	M-O bond strength	$TM^0/M(OH)_x$ redox potential	HOR mechanism	HER mechanism
Category 1	Cu@Pt	Weak	High (> 0.25 V)	Eley-Rideal	Eley-Rideal
Category 2	Co@Pt	Strong	Low (< ~0 V)	Eley-Rideal	HSAB
Category 3	Ru@Pt	Moderate	Moderate (~0-0.25 V)	L-H	HSAB